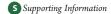


pubs.acs.org/est

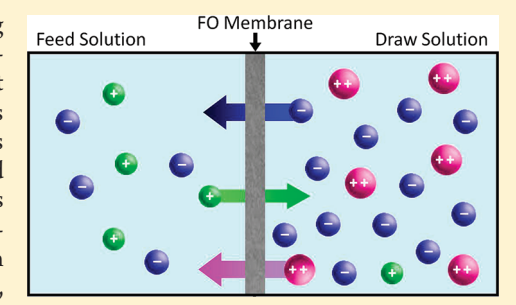
Bidirectional Permeation of Electrolytes in Osmotically Driven Membrane Processes

Nathan T. Hancock,[†] William A. Phillip,*,[‡] Menachem Elimelech,[§] and Tzahi Y. Cath*,[†]

- [†]Division of Environmental Science and Engineering, Colorado School of Mines, 1500 Illinois Street, Golden, Colorado 80401, United States
- [‡]Department of Chemical and Biomolecular Engineering, University of Notre Dame, 182 Fitzpatrick Hall, Notre Dame, Indiana 46556-5637, United States
- ^SDepartment of Chemical and Environmental Engineering, Yale University, P.O. Box 208286, New Haven, Connecticut 06520-8286, United States



ABSTRACT: Osmotically driven membrane processes (ODMP) are emerging water treatment and energy conversion technologies. In this work, we investigated the simultaneous forward and reverse (i.e., bidirectional) solute fluxes that occur in ODMP. Numerous experiments were conducted using ternary systems (i.e., systems containing three distinct ions) and quaternary systems (i.e., systems containing four distinct ions) in conjunction with a membrane in a forward osmosis orientation. Ten different combinations of strong electrolyte salts constitute the ternary systems; common anion systems studied included KCl-NaCl, KBr-NaBr, KNO₃-NaNO₃, KCl-CaCl₂, and KCl-SrCl₂; and common cation systems explored were KCl-KH₂PO₄, NaCl-NaClO₄, NaCl-Na₂SO₄, NaCl-NaNO₃, and CaCl₂-Ca(NO₃)₂. For each combination, two experiments



were conducted with each salt being used once in the draw solution and once in the feed solution. Quaternary systems studied were NaCl-KNO₃, NaCl-MgSO₄, MgSO₄-KNO₃, and NaCl-K₂SO₄. Experimental fluxes of the individual ions were quantified and compared to a set of equations developed to predict bidirectional electrolyte permeation for ODMP in a forward osmosis orientation. Results demonstrate that ion fluxes from the draw solution to the feed solution are well predicted; however, ion fluxes from the feed solution to the draw solution show slight deviations from the model that can be rationalized in terms of the electrostatic interactions between charged ions. The model poorly predicts the flux of nitrate containing solutions; however, several unique mass transfer mechanisms are observed with implications for ODMP process design.

■ INTRODUCTION

Osmotically driven membrane processes (ODMP), such as forward osmosis (FO), pressure retarded osmosis (PRO), and osmotic dilution, are an emerging class of technologies that may be used for water treatment^{1,2} and for sustainable energy generation.^{3,4} FO technology has demonstrated unique abilities to treat highly impaired water sources^{5–9} as well as to desalinate seawater and brackish water.^{10,11} The versatility of ODMP is partly due to their lower irreversible fouling propensity^{12–14} and to the spontaneity of mass transport that eliminates the need for operation with high hydraulic pressure.¹

Recent research to improve ODMP led to the development of new membranes with unique support structures that reduce the mass transfer limitations imposed by internal concentration polarization ^{15–18} and the exploration of novel draw solutions to enable treatment of highly saline feed streams. ¹⁰ However, fundamental problems related to the bidirectional transport of solutes through ODMP membranes require additional investigation to further improve the processes. Reverse permeation of solutes from the draw solution through the membrane into the

feed stream, in the opposite direction of the water flux, decreases the driving force for water permeation and may necessitate replenishment of the draw solution. Likewise, permeation of feed solutes through the membrane into the draw solution may negatively impact the performance of the downstream process. This may be especially acute when sparingly soluble salts accumulate and precipitate in systems that employ a closed-loop draw solution reconcentration process.

Previous studies^{5,19–24} examined the transport of solutes in FO. These studies identified the reverse permeation of draw solution solutes as a potential obstacle for future process design and implementation. Two recent studies^{19,25} found that the specific reverse flux (the inverse of reverse flux selectivity²⁰) through a cellulose triacetate (CTA) membrane into deionized water feed can vary by an order of magnitude between different

Received: July 27, 2011
Accepted: October 28, 2011
Revised: October 20, 2011
Published: October 28, 2011

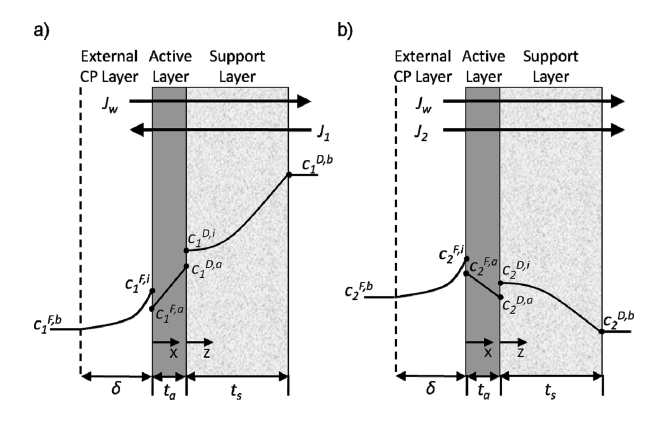


Figure 1. Schematics of concentration profiles for (a) the draw solution electrolyte and (b) the feed solution electrolyte. Local coordinates x and z are established with respect to the forward water flux (J_w) . Both electrolytes are transported down their concentration gradient resulting in a net reverse flux of draw solution electrolyte, J_1 , and a net forward flux of feed solution electrolyte, J_2 . Electrolytes must be transported across the external concentration polarization layer, active layer, and porous support layer with thickness δ , t_a , and t_s , respectively. Subscripts are used to denote either the draw solution electrolyte (1) or feed solution electrolyte (2). Superscripts represent the concentration of these ions at specific locations along their concentration profile, where F and D correspond to the feed and draw solution sides of the active layer, and b, i, and a correspond to the bulk solution, interface, or active layer, respectively.

draw solutions. A recent study²⁰ derived a model to predict the rate of reverse permeation of strong electrolytes (e.g., NaCl), and related the reverse flux selectivity of the membrane to the membrane electrolyte and solvent (water) permeabilities.

In another recent study¹⁹ we explored the bidirectional

In another recent study. We explored the bidirectional transport of solutes through membranes in FO. Solutes were observed to diffuse at different rates based primarily on the size of the hydrated molecule. Ions that form larger hydration shells (e.g., barium, magnesium, calcium) exhibited lower fluxes compared to ions with smaller hydration shells (e.g., potassium, sodium, ammonium). During all experiments, ions were observed to diffuse at rates that maintained electroneutrality, and Donnan effects were also observed. For example, in one set of experiments, a feed stream consisting of BaNO₃ was used. The highly mobile nitrate ion was able to permeate through the membrane at a substantially faster rate than barium. In this case, chloride from the NaCl draw solution was observed to permeate at a greater rate relative to sodium to maintain the electroneutrality of the solutions.

The objective of this study was to develop a comprehensive understanding of bidirecitonal solute permeation through the membrane during FO. Specifically, the potential impact of electrostatic interactions on the bidirectional permeation of ions through the membrane was explored using a combination of bench-scale experiments and phenomenological modeling. A series of ternary ion experiments with an inorganic electrolyte dissolved in the feed solution and another distinct electrolyte, but one which shares a common anion or cation, dissolved in the draw solution were conducted, and the flux of each ion was measured. The measured ion fluxes were compared to a model developed for electrolyte permeation in the absence of interactions between the draw solution and feed solution ions. Deviations between the model and experimental results were reconciled in terms of the electrostatic interactions that occur

between charged ions from the feed and draw solutions. A limited number of quaternary ion systems were explored to investigate what aspects of the model could be extended to higher order systems. Implications of the results for the design and operation of ODMPs are discussed.

■ THEORETICAL BACKGROUND

Forward and Reverse Fluxes of Noninteracting Electrolytes. In this study we are exploring how electrostatic interactions between ions can influence their forward and reverse permeation in FO. To begin, we derive expressions for the electrolyte fluxes, ignoring the electrostatic interactions between the constituent ions. Please note that we use the term electrolyte to refer to the parent salt that when dissolved in solution forms ions. A schematic of an asymmetric membrane operating in FO mode is shown in Figure 1.

The permeation of an electrolyte from the draw solution into the feed solution (Figure 1a) and an electrolyte from the feed solution into the draw solution (Figure 1b) requires their transport across three distinct regions: the external boundary layer, the dense active layer, and the porous support layer. Transport of electrolytes in the support layer and boundary layer occurs by both diffusion and convection, but only diffusion controls electrolyte transport through the active layer — consistent with the solution-diffusion transport mechanism. ^{28,29}

By writing mass balances on each of the layers and equating the electrolyte fluxes at the interfaces between the layers, expressions for the electrolyte fluxes in the absence of electrostatic interactions can be derived (eqs 1 and 2). The details of these derivations were previously reported³⁰ and are provided in the SI. Here we present the final results for the draw solution electrolyte and feed solution electrolyte fluxes, J_1 and J_2 , respectively

$$J_1 = \frac{J_w B_1(c_1^{F,b} \exp(Pe_1^F + Pe_1^D) - c_1^{D,b})}{(B_1 \exp(Pe_1^F) + J_w) \exp(Pe_1^D) - B_1}$$
(1)

$$J_2 = \frac{J_w B_2(c_2^{F,b} \exp(Pe_2^F + Pe_2^D) - c_2^{D,b})}{(B_2 \exp(Pe_2^F) + J_w) \exp(Pe_2^D) - B_2}$$
(2)

where J_w is the superficial fluid velocity (which is equivalent to the water flux), B_1 is the electrolyte permeability coefficient, $c_1^{F,b}$ is the concentration of draw solution electrolyte in the bulk feed solution, and $c_1^{D,b}$ is the concentration of draw solution electrolyte in the bulk draw solution. Pe_1^F and Pe_1^D are the Peclet numbers of the draw solution electrolyte in the external boundary layer and the support layer, respectively. These Peclet numbers quantify the relative importance of convective transport to diffusive transport in each layer and are defined as $Pe_1^F \equiv J_w/k$ for the external boundary layer, where k is the feed side mass transfer coefficient, and $Pe_1^D \equiv (J_w t_s \tau)/(D_{DS} \varepsilon)$ for the support layer, where D_{DS} is the bulk binary diffusion coefficient of the draw solution electrolyte and water, t_s is the support layer thickness, τ its tortuosity, and ε its porosity. All the variables have the same meaning in eq 2 but are now defined for the feed solution electrolyte instead of the draw solution electrolyte.

Equations 1 and 2 can be used to predict the reverse and forward electrolyte fluxes, respectively, in the absence of interactions between feed and draw solution electrolytes and will be used as a reference for comparison. Note that the electrolyte permeability and diffusion coefficients in these equations refer to

those measured for a single electrolyte where the fact that the electrolyte forms multiple ions when dissolved in solution has been ignored.²⁰ By doing so, the electrostatic interactions between the ions are ignored and electroneutrality is implicitly assumed. Below we consider these interactions more explicitly.

Effects of Electrostatic Interactions on Ion Permeation. In FO, ions from the feed and draw electrolytes will be present at appreciable concentrations within the dense active layer of the membrane. Therefore, it is important to understand how these ions are transported across the active layer and how they may interact with each other. Explicitly, considering that electrolytes form ions within the active layer of the membrane is particularly interesting. Our prior work with an NaCl draw solution and a deionized water feed solution demonstrated that the NaCl flux is linearly proportional to the NaCl concentration difference across the active layer. This result implies that the sodium and chloride permeate the active layer as charged ions and not an ion pair. Despite the evidence that ions permeate the active layer as two separate entities, their transport could be described by a single transport coefficient.

A Single Transport Coefficient Describes the Permeation of a Binary System. Dissolved solutes are transported through the dense active layer of the FO membrane by the solution-diffusion mechanism.²⁸ In this mechanism, the diffusing solute, which in the case of a dissolved electrolyte is the constituent cations and anions, must first partition into the active layer phase before diffusing across it. The partitioning of the cation and anion can be quantified using a Henry's-law-like constant, by assuming equilibrium at the active layer-aqueous solution interface

$$\mu_i^a = \mu_i^s \tag{3}$$

where μ_i is the chemical potential of species i, and the superscripts represent the phase: (a) active layer and (s) solution. The index of species i represents the specific ion in solution: 1 is an ion in the draw solution, 2 is an ion in the feed solution, and 3 is the counterion, which for ternary systems will be the common ion found in both the feed and draw solutions. For the binary case of a single 1:1 electrolyte, eq 3 can be written for each ion as follows

$$\mu_1^{a0} + RT \ln c_1^a + z_1 F \phi^a = \mu_1^{s0} + RT \ln c_1^s + z_1 F \phi^s$$
(4a)

$$\mu_3^{a0} + RT \ln c_3^a + z_3 F \phi^a = \mu_3^{s0} + RT \ln c_3^s + z_3 F \phi^s$$
(4b)

where μ_i^0 is a reference chemical potential, c_i is the concentration of species i, z_i is the valence, F is the Faraday constant, R is the ideal gas constant, T is the absolute temperature, and ϕ is the electrostatic potential. Adding eqs 4a and 4b, rearranging, and using the fact that for a 1:1 electrolyte $c_1 = c_3 = c$ yields

$$\frac{c^a}{c^s} = \sqrt{H_1 H_3} = H_{1/3} \tag{5}$$

where c is the electrolyte concentration, and H_{ij} the partition coefficient for the individual species i, is equal to

$$H_i = \exp\left(\frac{\Delta\mu_i^0}{RT}\right) \tag{6}$$

Therefore, the partition coefficient for the electrolyte (i.e., the coupled anion and cation), $H_{1/3}$, is the geometric average of the partition coefficient for each ion.²⁹

The extended Nernst—Planck equation can be used to demonstrate that the electrostatic coupling between the oppositely charged ions allows their motion to be described by a single diffusion coefficient. The flux of a charged species *i* defined by the extended Nernst—Planck equation is ²⁹

$$-J_{i} = D_{i} \left(\nabla c_{i} + z_{i} c_{i} \frac{F}{RT} \nabla \phi \right) \tag{7}$$

where J_i is the flux of species i, and D_i is the diffusion coefficient in the active layer. Additionally, the system must maintain electroneutrality, thus $\Sigma_i c_i z_i = 0$, and because there is no applied potential, the current, I, is equal to 0 (i.e., $I = \Sigma_i z_i J_i = 0$). This system of equations can be used to show that the diffusion coefficient of the 1:1 electrolyte in the active layer, $D_{1/3}$, is equal to the harmonic average of the ionic diffusion coefficients, D_1 and D_3

$$J_s = J_1 = J_3 = -\left(\frac{2D_1D_3}{D_1 + D_3}\right)\nabla c = -D_{1/3}\nabla c$$
 (8)

Equation 8 can be integrated over the active layer thickness, t_a . Then, using eq 5, the concentration difference can be written in terms of the electrolyte concentration in solution to yield the following expression for the flux across the active layer

$$J_s^a = \frac{D_{1/3} H_{1/3}}{t_a} \Delta c = B_{1/3} \Delta c \tag{9}$$

The group of terms $D_{1/3}H_{1/3}/t_a$ is more commonly measured and reported as the electrolyte permeability coefficient, $B_{1/3}$ (i.e., B_1 used in eq 1). Thus, a single coefficient can be used to quantify the flux of a binary (i.e., anion and cation) system.²⁹

Electrostatic Interactions Have a Small Effect on the Permeation of Ternary Systems. The electrostatic coupling between anion and cation of the binary system, which allows that system to be described by a single transport coefficient, may affect ion permeation in FO processes when ions from the feed solution interact with ions from the draw solution. We now consider a ternary system consisting of three ions with a common anion or cation in the feed and draw solution (e.g., an NaCl draw solution and a KCl feed or an NaCl draw solution and an NaClO₄ feed). A ternary system is used because analytical solutions do not exist for higher order systems. Multicomponent partitioning effects in ternary systems have been studied for cellulose acetate membranes designed for RO operations.³² In general, the observed effects were small. One important conclusion from these studies was that at operational pHs cellulose acetate membranes contain negligible fixed charged groups. Therefore, charges contained within the membrane will not have an observable effect on ion partitioning.³³

The Nernst-Planck equation, the electroneutrality constraint, and I = 0 are once again the starting points for deriving the transport coefficients. This system leads to²⁹

$$-J_i = D_{ij} \nabla c_j \tag{10a}$$

$$D_{ij} = \begin{bmatrix} D_1 + \frac{D_1 z_1^2 c_1 (D_3 - D_1)}{\sum\limits_{k=1}^{3} D_k z_k^2 c_k} & \frac{D_1 z_1 z_2 c_1 (D_3 - D_2)}{\sum\limits_{k=1}^{3} D_k z_k^2 c_k} \\ \frac{D_2 z_1 z_2 c_2 (D_3 - D_1)}{\sum\limits_{k=1}^{3} D_k z_k^2 c_k} & D_2 + \frac{D_2 z_2^2 c_2 (D_3 - D_2)}{\sum\limits_{k=1}^{3} D_k z_k^2 c_k} \end{bmatrix}$$

$$(10b)$$

where the diffusion coefficients D_{ij} quantify the proportionality between the flux of species i and the concentration gradient of species j. Equation 10b is written as a 2 × 2 matrix because the flux of the common ion (species 3) can be determined from the flux of the ion in the draw solution, J_1 , the flux of the ion in the feed solution, J_2 , and the fact that I = 0. By itself, eq 10b does not provide any clear physical insight into the bidirectional permeation of ions in FO. Therefore, it is helpful to consider what occurs when $c_1 \gg c_2$, a pertinent condition in FO where the draw solution concentration is much greater than the feed concentration. Under this condition, eq 10b reduces to

$$D_{ij} = \begin{bmatrix} \frac{(|z_1| + |z_3|)D_1D_3}{|z_1|D_1 + |z_3|D_3} = D_{1/3} & \frac{D_1z_2(D_3 - D_2)}{|z_1|D_1 + |z_3|D_3} \\ 0 & D_2 \end{bmatrix}$$
(11)

This provides much more physical insight into the transport of ions in FO. The cross-term D_{21} , which quantifies how much the flux of species 2 (the feed solution ion) is influenced by the gradient of species 1 (the draw solution ion), goes to 0. Therefore, the concentration gradient of the draw ion should not affect the flux of the feed ion, although the draw solution concentration must be high enough that the limit $c_1 \gg c_2$ is satisfied. The term D_{22} reduces to D_2 (i.e., the ionic diffusion coefficient of species 2), which implies that because there is excess of the common counterion (species 3) present, species 2 is able to permeate through the active layer at a rate independent of species 1 and 3. The ability of species 2 to permeate independently may produce some noticeable variations in its flux that can be observed during experiments; however, the difference between the ionic diffusion coefficients, D_2 and D_3 , is often negligible and any variations are likely to be small.

The diffusion coefficients for species 1 also yield interesting values under this condition $(c_1 \gg c_2)$. The cross-term D_{12} is nonzero because species 1 adjusts its permeation rate to allow species 2 to permeate at its independent rate, while still maintaining electroneutrality. The main term coefficient, D_{11} , reduces to $D_{1/3}$, which is equal to the weighted average of the ionic diffusion coefficients of ions 1 and 3 (i.e., eq 8). Examining the relative magnitudes of $D_{12}\nabla c_2$ and $D_{11}\nabla c_1$, it is easily shown that $D_{11}\nabla c_1$ will dominate the flux of species 1. Therefore, the electrostatic coupling between ions from the feed and draw solutions will have little effect on the flux of ions from the draw solution.

■ MATERIAL AND METHODS

Model Inorganic Salts. Thirteen ACS grade salts were used in this study: NaCl (Sigma-Aldrich/Fluka, Buchs, Switzerland); SrCl₂ and NaClO₄ (Sigma-Aldrich, St. Louis, MO); KH₂PO₄, KNO₃, Ca(NO₃)₂, and NaNO₃ (Fisher Scientific, El Monte, CA); Na₂SO₄, MgSO₄, NaBr, KCl, and CaCl₂ (Mallinckrodt Chemicals, Phillipsburg, NJ); and KBr (Spectrum Chemical Products, Gardena, CA). Ternary and quaternary ion experiments were conducted to explore the bidirectional fluxes of dissolved salts. Both ternary and quaternary experiments were conducted with a 1 M draw solution concentration and 0.05 M feed solution concentration, with the exception of a few experiments that are explicitly defined in the Results and Discussion section in which the concentrations were different.

Bench-Scale System Design. A bench-scale testing apparatus similar to that described in a previous publication was employed for this study. The testing cell was constructed with symmetric flow chambers, each containing two 575 mm \times 48 mm \times 1.6 mm (L \times W \times H) channels separated by a gasket. Draw and feed solutions were circulated cocurrently through the chambers at a flow rate of 2 L/min. A programmable logic control system was developed to maintain constant experimental conditions (i.e., feed volume of 3 L, draw solution concentration, and system temperature of 20 °C) and to collect experimental data. Details about the design and operation of the system are provided elsewhere. 30

Sampling and Analytical Methods. Samples of the feed and draw solutions were collected at the beginning of each experiment and after 1 and 2 L of water permeated through the FO membrane. Diluted samples were analyzed with ion chromatography (IC) (ICS-90, Dionex, Sunnyvale, CA) and inductively coupled plasma atomic emission spectroscopy (ICP-AES) (Optima 5300, Perkin-Elmer, Fremont, CA) to determine the concentration of anions and cations, respectively. Anion concentrations analyzed with IC were measured in duplicate with a typical relative standard deviation of 2.2%. Cation concentrations analyzed with ICP-AES were measured in triplicate with a typical relative standard deviation of 1.8%.

The mass of draw solution ions in the feed stream was recorded as a function of time and normalized by the membrane area to determine the reverse flux of draw solution ions. An identical process was followed to measure the forward flux of the feed solution ion.

Forward Osmosis Membrane Characterization. The membrane used for this study (Hydration Technology Innovations, Albany, OR) is similar to the CTA membranes used in previous studies. The membrane is believed to be composed of a cellulose triacetate layer with an embedded woven support mesh. Membrane integrity tests, using a 1 M NaCl draw solution and a Milli-Q deionized water feed, were routinely performed to ensure that membrane performance (i.e., water flux and reverse NaCl salt flux) were consistent between experiments. The membrane was replaced if either water or reverse NaCl salt flux deviated more than 5% from their established baseline values. The average water flux and reverse NaCl salt flux over 26 integrity tests were $10.2 \pm 0.35 \, \text{L/m}^2 \cdot \text{hr}$ and $127 \pm 9 \, \text{mmol/m}^2 \cdot \text{hr}$, respectively.

Pure water permeability (A) and the membrane structural parameter ($S \equiv t_s \tau/\epsilon$) were measured in FO mode (i.e., draw solution facing the support layer and no applied hydraulic pressure) using the method reported in a previous publication. Water flux was measured at three different draw solution concentrations (0.5, 1.0, and 1.5 M NaCl) with deionized water feed. Thermophysical modeling software (OLI Analyzer v3.0, OLI Systems Incorporated, Morris Plains, NJ) was employed to calculate the osmotic pressure of the draw solutions to account for the nonideality of concentrated solutions.

Two samples of the same commercial membrane were used during these experiments. The different samples had slightly different transport characteristics. The pure water permeability and structural parameter of Membrane I were determined to be 0.44 \pm 0.04 L/m²·hr·bar (1.36 \times 10 $^{-12}$ \pm 9.80 \times 10 $^{-14}$ m/Pa·s) and 439 \pm 26 μ m, respectively. Membrane II was more permeable but had a higher structural parameter ($A=0.52\pm0.02~{\rm L/m}^2\cdot{\rm hr}\cdot{\rm bar}$ (1.45 \times 10 $^{-12}\pm4.90\times10^{-14}$ m/Pa·s) and

Table 1. Water and Cation Fluxes Measured during PRO Mode Experiments and Characteristic Transport Coefficients^a

salt	$D_{DS}^{45} (10^{-9} \text{ m}^2/\text{s})$	$J_{w}\left(10^{-6}\;\mathrm{m/s}\right)$	$k (10^{-5} \text{ m/s})$	cation flux $(mmol/m^2 \cdot hr)$	$B (10^{-8} \text{ m/s})$
		Ŋ	Membrane I		
NaClO ₄	1.53	3.14	1.17	1297.8 ± 21.7	49.92
NaNO ₃	1.56	3.52	1.19	420.5 ± 10.1	16.28
$Ca(NO_3)_2$	1.29	5.18	1.05	74.5 ± 1.5	5.04
KBr	2.02	4.43	1.41	400.0 ± 4.3	16.19
NaBr	1.62	4.50	1.22	288.0 ± 2.8	12.56
KCl	1.99	4.35	1.40	190.4 ± 0.2	7.64
NaCl	1.61	3.79	1.25	156.7 ± 7.7	6.02
CaCl ₂	1.33	5.71	1.07	33.7 ± 0.7	2.38
$SrCl_2$	1.34	5.21	1.07	27.4 ± 1.8	1.99
KH_2PO_4	1.18	2.18	0.99	18.3 ± 4.4	1.26
Na_2SO_4	0.41	2.68	1.01	30.5 ± 2.9	1.72
		Ν	Membrane II		
KCl	1.99	4.89	1.40	521.6 ± 2.0	19.44
NaCl	1.61	4.75	1.25	280.4 ± 0.6	12.22
CaCl ₂	1.33	5.99	1.07	85.9 ± 1.7	4.17

^a The electrolyte diffusion coefficients in water were calculated using eq 8, the mass transfer coefficients were obtained from the correlation developed in ref 35, and the electrolyte permeation coefficients were determined using the method in ref 20. Salt pairs are listed in order from most chaotropic to most kosmotropic based on their anion.³⁷ The two membrane samples used in this work are listed as Membrane I ($A = 1.36 \times 10^{-12} \pm 9.80 \times 10^{-14}$ m/Pa·s; $S = 439 \pm 26 \ \mu m$) and Membrane II ($A = 1.45 \times 10^{-12} \pm 4.90 \times 10^{-14}$ m/Pa·s; $S = 559 \pm 42 \ \mu m$).

 $S = 559 \pm 42 \,\mu\text{m}$). These variations are similar to those observed in the published literature for this membrane. ^{20,34}

Additional experiments were conducted in PRO mode (i.e., draw solution facing the active layer and no applied hydraulic pressure) to determine the permeability coefficient (*B*) for various electrolytes using the method reported in a previous publication. ²⁰ In each experiment, the draw solution concentration of electrolyte was 1 M and the feed was deionized water. Samples were drawn at predetermined times throughout each experiment and analyzed with IC and ICP-AES. The flux of ions into the feed was calculated using the method reported above.

■ RESULTS AND DISCUSSION

Membrane Performance Parameters. Permeability coefficients, B, for the various electrolytes used in this study were determined from PRO mode experiments and are reported in Table 1. The electrolyte diffusion coefficient in water, ²⁹ observed water flux, mass transfer coefficient, ³⁵ and molar flux of the cation used in this calculation are also summarized in Table 1 (molar flux of the anions are provided in the SI). The rate that salts with similar cations permeate through the membrane correlates with their anion. Permeabilities were highest for perchlorate containing salts, and incrementally decreased in the order of nitrate, bromine, chloride, dihydrogen phosphate, and sulfate containing salts. Empirically, this follows a similar trend as the Hofmeister series. $^{36-38}$

A trend in the permeability coefficients for the electrolytes with similar anions can also be seen in Table 1. Salts containing divalent cations diffuse more slowly than salts with similar anions that contain monovalent cations. Among monovalent cations, diffusion rates are consistently greater for salts containing potassium instead of sodium. This behavior is in accordance with previous observations^{19,25,29,39} and indicates that a smaller hydration radius correlates to faster permeation through the membrane.

Model Validation of Experimental Water Flux. Experiments were conducted in FO mode to measure the water flux and bidirectional flux of ions. Ten combinations of salts were used in 18 different experiments. Measured water fluxes from these experiments were compared to predicted values from existing models^{34,40,41} (Figure 2). In many cases, the water flux was under predicted but was within 10% of perfect agreement. Predicted water flux values were used in eqs 1 and 2 to calculate the forward and reverse flux of electrolytes *a priori*.

Ion Permeation in Common Anion Systems. Experiments were performed using ternary systems that share a common anion in the feed and draw solutions. The experimentally determined ion fluxes are compared to the predicted fluxes calculated from eqs 1 and 2. One of the goals of this work is to explore the impact of electrostatic interactions on the bidirectional flux of ions in ODMP; thus, the predicted cation fluxes were calculated using the electrolyte permeability coefficients in Table 1. The model used has already been validated for single salt systems, ²⁰ meaning any significant deviations between the predicted and experimental ion fluxes are indicative of differences that arise from the presence of another ion. The predicted anion fluxes can be found by taking the sum of the predicted cation fluxes.

The predicted and measured fluxes are compared on log—log plots in Figure 3a and b, where the systems have been separated by the relative mobility of the draw electrolyte based on the permeability coefficients, *B*. Results from experiments with the more mobile cation in the draw solution are shown in Figure 3a, and results from common anion experiments with the more mobile cation in the feed solution are shown in Figure 3b. Water flux, cation and anion fluxes, and experimental error data for all the systems studied are provided in the SI.

The molar fluxes of ions from the draw solution into the feed solution are clustered in the top right region of both panels (Figure 3a and b). As expected, these fluxes are higher than the

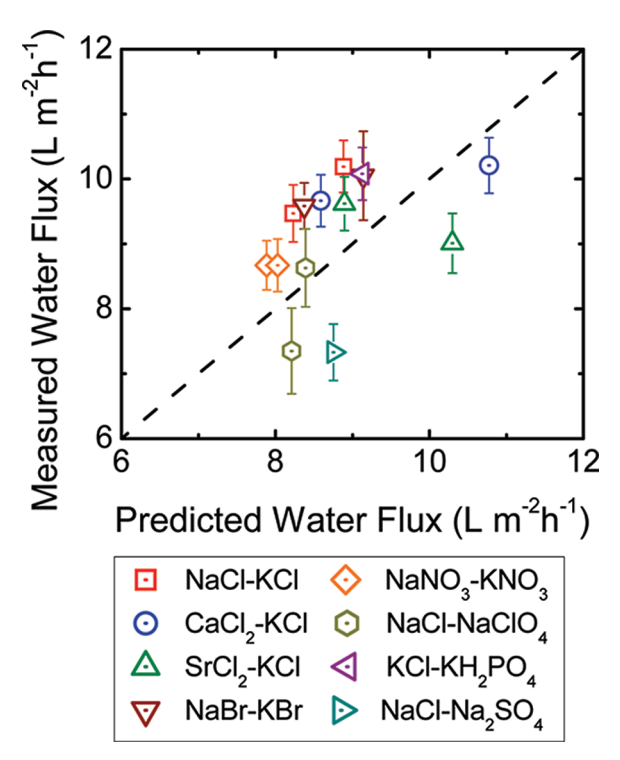


Figure 2. Comparison of the observed water flux to the predicted water flux for ternary electrolyte experiments. The predicted water fluxes are calculated using equations derived in previous studies. 34,40 The aqueous diffusion coefficient, D, and feed side mass transfer coefficient, k, for each salt are reported in Table 1, $S=439~\mu m$, and $A=0.44~L~m^{-2}~h^{-1}~bar^{-1}$. The dashed line (slope = 1 represents perfect agreement between predicted water flux values and those observed from experiments. Two water fluxes are reported for each system of electrolytes because each salt was used once as in the draw solution and once in the feed solution. Only one data point is reported for the KH₂PO₄ and Na₂SO₄ containing systems because neither salt was soluble enough to prepare a 1.0 M draw solution. Error bars represent one standard deviation.

feed ion flux for a given experiment. ^{19,20,25,42} In the ternary systems, the draw solution ion fluxes are predicted by eqs 1 and 2 with relative accuracy as demonstrated by the close proximity of data points to the line with slope = 1 (i.e., perfect agreement) in Figure 3a and b. One critique of the model (eq 2) is that it may slightly overpredict the flux of the cation in the feed solution (shown in the lower left quadrant and central region of Figure 3a and b, respectively). Analytical error associated with sample preparation and analysis may partially account for this deviation. Yet, this observation may also indicate that the feed cation is permeating through the active layer at a different rate due to the presence of a high concentration of the draw solution ions, as discussed in the interpretation of eq 11. Additional experiments were performed to further explore this observation.

The $CaCl_2$ draw solution and KCl feed solution system was selected for further experiments because this system showed the greatest deviations from the model predictions. Experiments were conducted using a $CaCl_2$ draw solution concentration between 0.5 and 2.0 M and a 0.05 M KCl feed solution. Membrane II, which was observed to have slightly different permeabilities and structural parameter (Table 1), was used during this portion of the investigation. The molar flux of potassium as a function of $CaCl_2$ concentration is presented in Figure S1.

Results from experiments show that the flux of potassium ions is independent of the CaCl₂ concentration gradient, which is in agreement with the limit presented in eq 11. Furthermore, the measured flux of potassium is consistently lower than the flux predicted by eq 2, which seems to indicate that the presence of the concentrated draw solution enables the feed ion to permeate through the membrane active layer at a rate set by the ionic permeability of potassium, not the potassium chloride permeability. Again, this is consistent with eq 11. An experiment was also performed with a 1 M CaCl₂ draw solution and a 0.15 M KCl feed solution to demonstrate that the flux of potassium does increase when the KCl feed concentration increases. Reassuringly, a 3-fold increase in KCl concentration lead to a corresponding increase in potassium flux (11.3 mmol m⁻² hr⁻¹ to 34.2 mmol $m^{-2} hr^{-1}$). The flux of calcium ions from the draw solution into the feed remained constant when the KCl concentration changed (26.4 mmol m⁻² hr⁻¹ at 0.05 M KCl and 27.0 mmol m⁻² hr⁻¹ at 0.15 M KCl). Taken together, these results suggest that if only electrostatic interactions exist between ions from the feed solution and draw solution (i) the flux of ions from the draw solution into feed solution will not be affected by the presence of ions from the feed solution and (ii) the flux of ions from the feed solution into the draw solution will be slightly affected due to the high concentration of draw solution ions.

Ion Permeation in Common Cation Systems. Ternary ion experiments were also performed with solutions that contain common cations and dissimilar anions. The predicted and measured ion fluxes are compared on log-log plots in Figure 4a and b. Experiments are divided into two groups: those performed with salts that do not contain nitrate (Figure 4a) and those that do contain nitrate (Figure 4b). Similar to results in Figure 3a and b, the molar fluxes of ions from the draw solution into the feed solution are clustered in the top right region of both figures, while the feed anion data points occupy the central and bottom left regions. For systems that did not contain nitrate, the experimental fluxes of ions from the draw solution were well predicted by the application of eqs 1 and 2 and the permeability coefficients in Table 1. Forward feed ion fluxes again deviated from those predicted by eq 2, although in this case the fluxes were slightly underpredicted.

The observation that the feed anions in common cation systems permeate more quickly than predicted while the feed cations in common anion systems permeate more slowly is consistent with the knowledge that ionic diffusion coefficients of anions tend to be higher than those of cations. Therefore, because the high draw solution concentrations enable the feed solution ions to permeate independently, the cations "slow down" and the anions "speed up" relative to the electrolyte permeability coefficient.

The ion fluxes in common cation experiments with nitrate containing salts (Figure 4b) are poorly predicted by eqs 1 and 2. It is possible that this is because interactions between the polar structure of nitrate and the membrane increase the nitrate partitioning into the membrane. We are currently pursuing further understanding of the mechanism of nitrate permeation through the membrane.

Ion Permeation in Quaternary Systems. Feed streams will typically contain a large number of dissolved ions; however, analytical solutions to the Nernst—Planck equation only exist for systems containing up to three ions. In order to explore what aspects of the understanding developed from the analytical solution (eq 11) might be extended to higher order systems, a

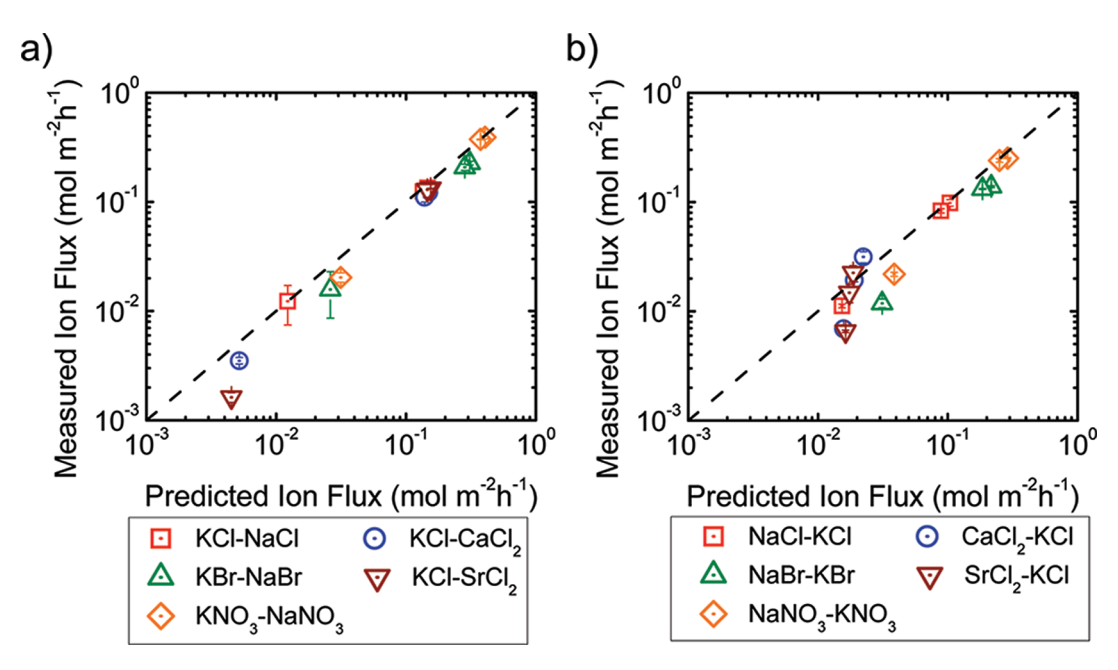


Figure 3. Comparison of the observed ion fluxes to the predicted ion fluxes for common anion systems. The systems are divided into two categories: (a) those with the more mobile cation in the draw solution and (b) those with the more mobile cation in the feed solution. Predicted ion fluxes are calculated using eqs 1 and 2 along with the predicted water fluxes, J_{100} , reported in Figure 2. The transport parameters D, B, and B correspond to those reported in Table 1 for Membrane I, and B = 439 μm. In the legend, the first salt is for the draw solution (1.0 M), and the second salt is for the feed solution (0.05 M) (e.g., NaCl-KCl refers to an experiment using a 1.0 M NaCl draw solution and a 0.05 M KCl feed solution). Three ion fluxes are reported for each experiment: the fluxes of the two distinct cations and the flux of the shared common anion. The dashed line (slope = 1) represents perfect agreement between predicted ionic fluxes and those measured from experiments. Error bars represent one standard deviation.

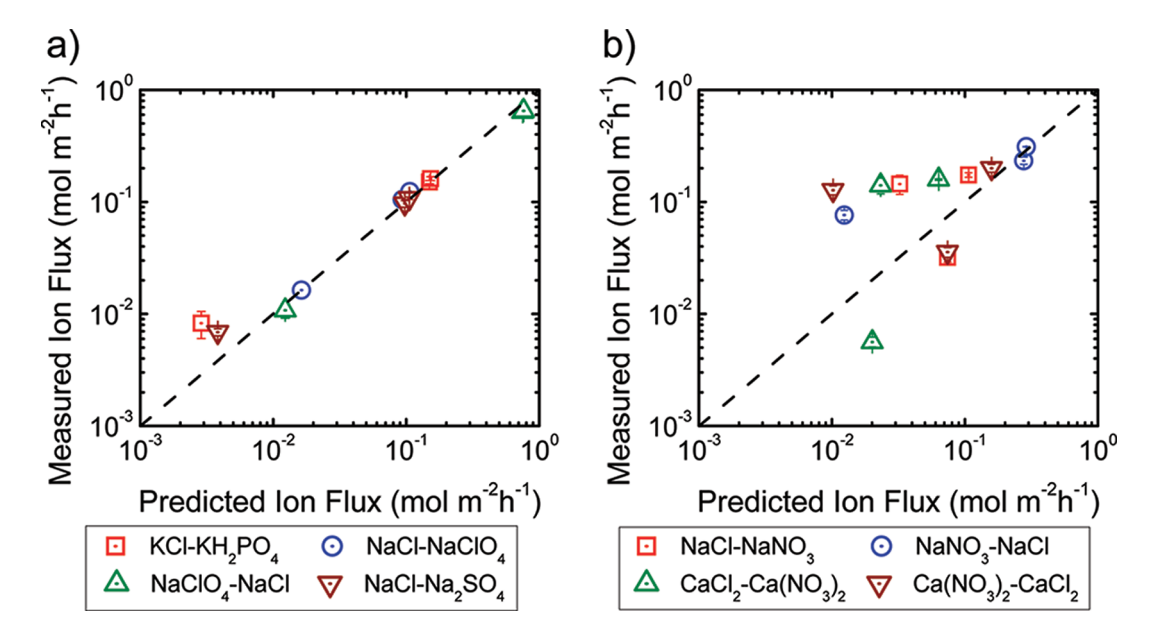


Figure 4. Comparison of the observed ion fluxes to the predicted ion fluxes for common cation ternary electrolyte systems. The systems are separated into two categories: (a) systems that *do not* use nitrate containing salts and (b) systems that *do* use nitrate containing salts. Predicted ion fluxes are calculated using eqs 1 and 2 and the predicted water fluxes, J_{w} , are reported in Figure 2. The transport parameters D, B, and B correspond to those reported in Table 1 for Membrane I, and B = 439 μ m. In the legend, the first salt is for the draw solution (1.0 M) and the second salt is for the feed solution (0.05 M). Three ion fluxes are reported for each experiment: the fluxes of the two distinct anions and the flux of the shared common cation. The dashed line (slope = 1) represents perfect agreement between predicted ionic fluxes and those observed during experiments. Error bars represent one standard deviation.

limited number of experiments were conducted to investigate bidirectional ion permeation in quaternary systems (i.e., two distinct ions in the feed and another two distinct ions in the draw solution). Three experiments were conducted, and a fourth was adopted from our previous study. ¹⁹ Detailed quantitative results are provided in the SI.

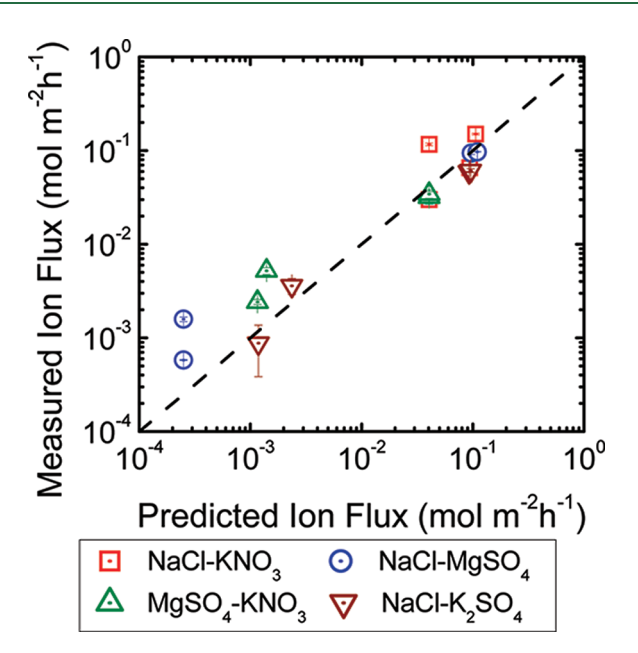


Figure 5. Comparison of the observed ion fluxes to the predicted ion fluxes for quaternary electrolyte systems. Predicted ion fluxes are calculated using eqs 1 and 2, and the predicted water fluxes, J_w , are reported in the SI. The transport parameters D, B, and k correspond to those reported in Table 1, and $S=439~\mu m$. In the legend, the experiments are identified using the same naming convention as that in Figures 3 and 4. Four ion fluxes are reported for each experiment because each dissolved salt produces two distinct ions. Please note that two symbols for the NaCl-KNO3 system are obscured by symbols from other systems. Both are located in the upper right-hand corner: one is located behind upward facing triangles of the MgSO4–KNO3 system and the other behind the downward facing triangles of the NaCl-K2SO4 system. The solid line (slope = 1) represents perfect agreement between predicted ionic fluxes and those observed from experiments. Error bars represent one standard deviation.

Similar to the ternary experiments, water flux in each experiment was predicted using established equations to within 10% of the observed values for these experiments (data not shown). Measured ion fluxes were compared to the fluxes predicted by eqs 1 and 2, assuming that the individual ions permeate at a rate set by the electrolyte permeability coefficient of their parent salts (Table 1). The predicted and measured ion fluxes are compared on a log-log plot shown in Figure 5. The observed results from these experiments are consistent with behaviors identified in the ternary experiments. For systems that do not contain nitrate, the predicted reverse flux of draw solution ions strongly agrees with the observed values. This indicates that electrostatic interactions between ions have a negligible effect on the reverse permeation of the draw electrolyte. The model predictions of the feed ion fluxes (eq 2) slightly deviate from experiments for these two cases, as we also observed in the ternary systems. For systems that contain nitrate, the model is unable to accurately predict the ion fluxes for the NaCl draw solution and KNO3 feed experiment. Deviations between the model and experiment are more noticeable when an NaCl draw solution is used compared to an MgSO₄ draw solution.

The development of osmotically driven membrane processes requires that a variety of complex phenomena be understood. One of those phenomena, the bidirectional permeation of ions, was thoroughly explored here through modeling and experimental efforts. Therefore, it is useful to consider how the results

of these efforts can aid the future development of ODMPs. Specifically, the experiments here demonstrate that solute solute (e.g., electrostatic) interactions do exist in the application of ODMPs and do affect the ionic fluxes through the membrane. These effects may be significant as is the case with nitrate containing systems or they may be much less important as is the case with electrostatic interactions. If only electrostatic interactions between charged species exists, the model developed here along with the electrolyte permeability coefficients measured from binary systems should adequately predict the reverse and forward ion fluxes in ODMPs. The model predictions will be very accurate for the reverse ion fluxes but less accurate for the forward ion fluxes because of the electrostatic interaction between ions. However, we suspect these differences will be negligible compared to some issues faced in the operation of field systems such as feed stream variability.44

ASSOCIATED CONTENT

Supporting Information. Details on the derivation of the bidirectional solute permeation model; tabulated experimental results including water flux, solute flux, and experimental error from binary, ternary, and quaternary systems. This material is available free of charge via the Internet at http://pubs.acs.org.

■ AUTHOR INFORMATION

Corresponding Author

*E-mail: wphillip@nd.edu (W.A.P.), tcath@mines.edu (T.Y.C.).

ACKNOWLEDGMENT

We acknowledge the support of California Department of Water Resources (Grant 46-7446-R-08), the AWWA Abel Wolman Fellowship, and Oasys Water Inc. Special thanks to Hydration Technology Innovations for providing the membrane utilized in this study.

■ NOMENCLATURE

A	water	permeabilit	y c	coefficien	t

B electrolyte permeability coefficient

c molar concentration of electrolyte c_i molar concentration of species i

 D_{DS} bulk diffusion coefficient of electrolyte in water

 D_{ij} diffusion coefficient of species i when influenced by gradient of species j

 $D_{i/j}$ average of diffusion coefficient of ions i and j

F Faraday constant

 H_i partition coefficient of species i

 $H_{i/i}$ average partition coefficient of ions *i* and *j*

I current density

 J_i molar flux of species i

 J_w volumetric water flux

k external mass transfer coefficient

R ideal gas constant

S membrane structural parameter

T absolute temperature

 t_a thickness of active layer

 t_s thickness of support layer

x, z local coordinate systems

 z_i valence of species i

- δ thickness of external concentration polarization layer
- ε porosity of support layer
- φ electrostatic potential
- μ_i chemical potential of species i
- π osmotic pressure
- *τ* tortuosity of support layer

■ SUBSCRIPTS

- refers to species originating from the draw solution (electrolyte or ion)
- 2 refers to species originating from the feed solution (electrolyte or ion)
- 3 refers to the counterion to ions 1 and 2; in ternary experiments, it is the common ion

■ REFERENCES

- (1) Cath, T. Y.; Childress, A. E.; Elimelech, M. Forward osmosis: principles, applications, and recent developments. *J. Membr. Sci.* **2006**, 281 (1–2), 70–87.
- (2) McGinnis, R. L.; Elimelech, M. Global Challenges in Energy and Water Supply: The Promise of Engineered Osmosis. *Environ. Sci. Technol.* **2008**, 42 (23), 8625–8629.
 - (3) Loeb, S. Osmotic power plants. Science 1974, 189, 350.
- (4) Yip, N. Y.; Tiraferri, A.; Phillip, W. A.; Schiffman, J. D.; Hoover, L. A.; Kim, Y. C.; Elimelech, M. Thin-Film Composite Pressure Retarded Osmosis Membranes for Sustainable Power Generation from Salinity Gradients. *Environ. Sci. Technol.* **2011**, *45* (10), 4360–4369.
- (5) Achilli, A.; Cath, T. Y.; Marchand, E. A.; Childress, A. E. The forward osmosis membrane bioreactor: A low fouling alternative to MBR processes. *Desalination* **2009**, 239, 10–21.
- (6) Cartinella, J. L.; Cath, T. Y.; Flynn, M. T.; Miller, G. C.; Hunter, K. W.; Childress, A. E. Removal of natural steroid hormones from wastewater using membrane contactor processes. *Environ. Sci. Technol.* **2006**, 40 (23), 7381–7386.
- (7) Cath, T. Y.; Gormly, S.; Beaudry, E. G.; Michael, T. F.; Adams, V. D.; Childress, A. E. Membrane contactor processes for wastewater reclamation in space: Part I. Direct osmosis concentration as pretreatment for reverse osmosis. *J. Membr. Sci.* **2005**, 257 (1–2), 85–98.
- (8) Cath, T. Y.; Hancock, N. T.; Lundin, C. D.; Hoppe-Jones, C.; Drewes, J. r. E. A multi-barrier osmotic dilution process for simultaneous desalination and purification of impaired water. *J. Membr. Sci.* **2010**, 362 (1–2), 417–426.
- (9) Holloway, R. W.; Childress, A. E.; Dennett, K. E.; Cath, T. Y. Forward osmosis for concentration of centrate from anaerobic digester. *Water Res.* **2007**, *41*, 4005–4014.
- (10) McCutcheon, J. R.; McGinnis, R. L.; Elimelech, M. A novel ammonia-carbon dioxide forward (direct) osmosis desalination process. *Desalination* **2005**, *174*, 1–11.
- (11) Martinetti, C. R.; Cath, T. Y.; Childress, A. E. High recovery of concentrated RO brines using forward osmosis and membrane distillation. *J. Membr. Sci.* **2009**, 331, 31–39.
- (12) Mi, B.; Elimelech, M. Organic fouling of forward osmosis membranes: Fouling reversibility and cleaning without chemical reagents. *J. Membr. Sci.* **2010**, 348 (1-2), 337–345.
- (13) Lee, S.; Boo, C.; Elimelech, M.; Hong, S. Comparison of fouling behavior in forward osmosis (FO) and reverse osmosis (RO). *J. Membr. Sci.* **2010**, 365 (1-2), 34–39.
- (14) Lay, W. C. L.; Chong, T. H.; Tang, C. Y. Y.; Fane, A. G.; Zhang, J. S.; Liu, Y. Fouling propensity of forward osmosis: Investigation of the slower flux decline phenomenon. *Water Sci. Technol.* **2010**, *61*, 927–936.
- (15) Yip, N. Y.; Tiraferri, A.; Phillip, W. A.; Schiffman, J. D.; Elimelech, M. High Performance Thin-Film Composite Forward Osmosis Membrane. *Environ. Sci. Technol.* **2010**, 44 (10), 3812–3818.
- (16) Zhang, S.; Wang, K. Y.; Chung, T.-S.; Chen, H.; Jean, Y. C.; Amy, G. Well-constructed cellulose acetate membranes for forward

- osmosis: Minimized internal concentration polarization with an ultrathin selective layer. *J. Membr. Sci.* **2010**, 360(1-2), 522-535.
- (17) Tiraferri, A.; Yip, N. Y.; Phillip, W. A.; Schiffman, J. D.; Elimelech, M. Relating performance of thin-film composite forward osmosis membranes to support layer formation and structure. *J. Membr. Sci.* **2011**, 367 (1-2), 340-352.
- (18) Bui, N.; Lind, M. L.; Hoek, E. M. V.; McCutcheon, J. R. Electrospun Nanofiber Supported Thin Film Composite Membranes for Engineered Osmosis. *J. Membr. Sci.* **2011**, DOI: (doi:10.1016/j.memsci.2011.08.002).
- (19) Hancock, N. T.; Cath, T. Y. Solute coupled diffusion in osmotically driven membrane processes. *Environ. Sci. Technol.* **2009**, 43, 6769–6775.
- (20) Phillip, W. A.; Yong, J. S.; Elimelech, M. Reverse Draw Solute Permeation in Forward Osmosis: Modeling and Experiments. *Environ. Sci. Technol.* **2010**, 44 (13), 5170–5176.
- (21) Xiao, D.; Tang, C. Y.; Zhang, J.; Lay, W. C. L.; Wang, R.; Fane, A. G. Modeling salt accumulation in osmotic membrane bioreactors: Implications for FO membrane selection and system operation. *J. Membr. Sci.* **2011**, 366(1-2), 314-324.
- (22) Cornelissen, E. R.; Harmsen, D.; de Korte, K. F.; Ruiken, C. J.; Qin, J.-J.; Oo, H.; Wessels, L. P. Membrane fouling and process performance of forward osmosis membranes on activated sludge. *J. Membr. Sci.* **2008**, 319 (1–2), 158–168.
- (23) Jin, X.; Tang, C. Y.; Gu, Y.; She, Q.; Qi, S. Boric Acid Permeation in Forward Osmosis Membrane Processes: Modeling, Experiments, and Implications. *Environ. Sci. Technol.* **2011**, 45 (6), 2323–2330.
- (24) Yaroshchuk, A. Influence of osmosis on the diffusion from concentrated solutions through composite/asymmetric membranes: Theoretical analysis. *J. Membr. Sci.* **2010**, *355* (1–2), 98–103.
- (25) Achilli, A.; Cath, T. Y.; Childress, A. E. Selection of inorganic-based draw solutions for forward osmosis applications. *J. Membr. Sci.* **2010**, 364 (1-2), 233–241.
- (26) Nightingale, E. R. Phenomenological theory of ion solvation. Effective radii of hydrated ions. *J. Phys. Chem.* **1959**, *63* (9), 1381–1387.
- (27) Donnan, F. G. The Theory of Membrane Equilibria. *Chem. Rev.* **1924**, *1* (1), 73–90.
- (28) Paul, D. R. Reformulation of the solution-diffusion theory of reverse osmosis. *J. Membr. Sci.* **2004**, 241 (2), 371–386.
- (29) Cussler, E. L. Diffusion mass transfer in fluid systems, 3rd ed.; University Press: Cambridge, 2009.
- (30) Hancock, N. T. Engineered Osmosis: Assessment of Mass Transport and Sustainable Hybrid System Configurations for Desalination and Water Reclamation. Colorado School of Mines, Golden, 2011.
- (31) Reusch, C. F.; Cussler, E. L. Selective Membrane Transport. *AIChE J.* **1973**, *19* (4), 736–741.
- (32) Heyde, M. E.; Anderson, J. E. Ion sorption by cellulose acetate membranes from binary salt solutions. *J. Phys. Chem.* **1975**, 79 (16), 1659–64.
- (33) Paul, D. R.; Geise, G. M.; Lee, H. S.; Miller, D. J.; Freeman, B. D.; Mcgrath, J. E. Water Purification by Membranes: The Role of Polymer Science. *J. Polym. Sci., Part B: Polym. Phys.* **2010**, 48 (15), 1685–1718.
- (34) McCutcheon, J. R.; Elimelech, M. Influence of concentrative and dilutive internal concentration polarization on flux behavior in forward osmosis. *J. Membr. Sci.* **2006**, 284 (1-2), 237–247.
- (35) Hoek, E. M. V.; Kim, A. S.; Elimelech, M. Influence of crossflow membrane filter geometry and shear rate on colloidal fouling in reverse osmosis and nanofiltration separations. *Environ. Eng. Sci.* **2002**, *19* (6), 357–372.
- (36) Hofmeister, F. Zur Lehre von der Wirkung der Salze [Title translation: About the science of the effect of salts]. *Arch. Exp. Pathol. Pharmakol.* **1888**, 24, 247–360.
- (37) Zhang, Y.; Cremer, P. S. Interactions between macromolecules and ions: the Hofmeister series. *Curr. Opin. Chem. Biol.* **2006**, *10*, 658–663.

- (38) Kunz, W.; Lo Nostro, P.; Ninham, B. W. The present state of affairs with Hofmeister effects. *Curr. Opin. Colloid Interface Sci.* **2004**, 9 (1-2), 1-18.
- (39) Mallevialle, J.; Odendaal, P. E.; Wiesner, M. R. Water treatment membrane processes; McGraw-Hill: USA, 1996.
- (40) Mehta, G. D.; Loeb, S. Internal polarization in the porous substructure of a semi-permeable membrane under pressure-retarded osmosis. *J. Membr. Sci.* **1978**, *4*, 261.
- (41) Loeb, S.; Titelman, L.; Korngold, E.; Freiman, J. Effect of porous support fabric on osmosis through a Loeb-Sourirajan type asymmetric membrane. *J. Membr. Sci.* 1997, 129, 243–249.
- (42) Robinson, R. A.; Stokes, R. H. Electrolyte Solutions: the measurement and interpretation of conductance, chemical potential, and diffusion in solutions of simple electrolytes, 2nd ed. (revised) ed.; Buttersworths Scientific Publications: London, 1959.
- (43) Paugam, L.; Taha, S.; Dorange, G.; Joauen, P.; Quemeneur, F. Mechanism of nitrate ions transfer in nanofiltration depending on pressure, pH, concentration and medium composition. *J. Membr. Sci.* **2004**, 231, 37–46.
- (44) Christofides, P. D.; Zhu, A. H.; Cohen, Y. Energy Consumption Optimization of Reverse Osmosis Membrane Water Desalination Subject to Feed Salinity Fluctuation. *Ind. Eng. Chem. Res.* **2009**, 48 (21), 9581–9589.
- (45) Li, Y.; Gregory, S. Diffusion of ions in seawater and in deep-sea sediments. *Geochim. Cosmochim. Acta* **1974**, *38*, 703–714.